Eur. Phys. J. B **20**, 303–311 (2001)

THE EUROPEAN PHYSICAL JOURNAL B

EDP Sciences

The two-dimensional t-t'-U model as a minimal model for cuprate materials

A. Avella[1,a], F. Mancini[1], D. Villani[1], and H. Matsumoto[2]

[1] Dipartimento di Fisica "E.R. Caianiello" - Unità INFM di Salerno, Università degli Studi di Salerno, 84081 Baronissi (SA), Italy
[2] Department of Applied Physics, Seikei University, Tokyo 180, Japan

Received 29 March 2000 and Received in final form 10 August 2000

Abstract. The addition to the Hubbard Hamiltonian of a t' diagonal hopping term, which is considered to be material dependent for high-T_c cuprate superconductors, is generally suggested to obtain a model capable to describe the physics of high-T_c cuprate materials. In this line of thinking, the two-dimensional *t-t'-U* model has been studied by means of the Composite Operator Method, which allows to determine the dynamics in a fully self-consistent way by use of symmetry requirements, as the ones coming from the Pauli principle. At first, some local quantities have been calculated to be compared with quantum Monte Carlo data. Then, the structure of the energy bands, the shape of the Fermi surface and the position of the van Hove singularity have been computed as functions of the model parameters and studied by the light of the available experimental data. The results of our study show that there exists two sets of parameters that allows the model to describe the relevant features of the 1-layer compounds $Nd_{2-x}Ce_xCuO_4$ and $La_{2-x}Sr_xCuO_4$. On the other hand, for the 2-layer compound $YBa_2Cu_3O_{7-\delta}$ is not possible to find a reasonable set of parameters which could reproduce the position of the van Hove singularity as predicted by ARPES experiments. Hence, it results questionable the existence of an unique model that could properly describe the variety of cuprate superconductors, as the two-dimensional *t-t'-U* model was thought to be.

PACS. 71.10.Fd Lattice fermion models (Hubbard model, etc.) – 71.10.w Theories and models of many-electron systems – 71.27.+a Strongly correlated electron systems: heavy fermions

1 Introduction

Since the discovery of high-T_c superconductivity there has been a great deal of discussion about the choice of an effective model suitable to describe the properties of the copper-oxide planes in the perovskite structure. Extensive studies of the magnetic properties, showing one spin degree of freedom in the Cu-O plane [1], have resulted in considerable evidence that the high-temperature superconductors may be modeled by an effective single-band model. According to this, one of the most studied model is the single-band Hubbard model which indeed can qualitatively describe many physical properties experimentally observed in copper-oxide compounds.

The addition of a finite t' diagonal hopping term, that appears to be material dependent for high-T_c cuprate superconductors, has often been suggested to handle the complexity of the experimental situation for the cuprates [2–4]. Moreover, an electron-hole asymmetry in the next-nearest-neighbor hopping term, combined with a perfect symmetry of all the other effective parameters, emerges from various reduction procedures of multicomponent electronic models and seems to distinguish the cuprates from a general charge-transfer insulator [5,6]. It has been argued that this asymmetry is responsible for the stabilization (destabilization) of antiferromagnetic order for electron doping (hole doping) [7], whereas the spatial distribution of the doped carriers [8] and the damping of quasi particles [9] have been shown to be very sensitive to the sign of t'. A finite t' has been found to be essential in reproducing various experiments (magnetic structure factor [10,11], flat quasi particle dispersion and shape of the Fermi surface [12] which in turn are responsible for various anomalous normal state properties, sign change in the Hall effect [13], photoemission data [14], the behavior of the resistivity with temperature [14], the symmetry of the pairing state [15], the actual value of the critical temperature for the optimal doping concentration [5,6]). In addition, the sign of t' seems to be relevant for the thermodynamics, in agreement with more general arguments [16] that the propagation within one sublattice without spin flip allowed by a non zero t' would significantly change the physics. Therefore, the next-nearest-neighbor hopping

[a] e-mail: avella@sa.infn.it

parameter t' emerges as the single parameter, which carries, at the level of the single band description, the information about crystal structure outside the Cu-O planes and thus differentiates between the various cuprates [5,6].

According to this, we have decided to study the two-dimensional *t-t'-U* model to analyze if it could properly describe the variety of cuprate superconductors.

In recent years much attention has been paid to the physics of electronic systems (*e.g.*, cuprates, manganites, heavy fermions) with unconventional metallic properties. It is generally believed that the origin of this anomalous metallic behavior is due to strong electron correlations in narrow conduction bands [17]. In this line of thinking many analytical methods have been developed for the study of strongly correlated electron systems [18]. A parallel approach to the study of these systems is based on the use of numerical methods [15]. The numerical techniques are now very well developed and many results on finite-dimension lattices are available; these results are certainly a guide for the construction of a microscopical theory and to them in any case the different theoretical formulations must refer.

In the last years we have been developing a method of calculation, denominated Composite Operator Method [19–25] (COM), which has been revealed to be a powerful tool for the description of local and itinerant excitations in strongly correlated electronic systems. The method is based on the observation that the original field operators, in terms of which the interacting Hamiltonians are expressed, are not a convenient basis. Then, a crucial point is the identification of a set of composite operators that could describe the quasi-stable excitations which are supposed to be present in the system. The choice of a non-standard operator basis generates some parameters not directly connected to the single particle Green's function. Unlikely other approaches, the presence of these parameters is not inconvenient because it opens the possibility to bind the dynamics in a suitable Hilbert space, reabsorbing the symmetries which might be lost when some approximations are made. In particular, by using relations with the content of the Pauli principle [19,20], we are allowed to fix the dynamics of the system in a fully self-consistent way without recurring to factorization or other procedures [26–28]. In a physics dominated by the interplay between the charge and the magnetic configurations, we think that the Pauli principle should play an important role. Furthermore, the recovery of the Pauli principle, usually violated by other approximations, assures us that the hole-particle symmetry is satisfied and that the dynamics is bound to the right Hilbert space. In fact, the symmetry dictated by the Pauli principle and that coming from the hole-particle symmetry are intimately connected, so that the violation of the former implies the violation of the latter, and *vice versa* [20]. In this paper, we apply the method to the *t-t'-U* model; preliminary results have been given in reference [29], to which we will often refer, and the study of the magnetic properties have been given in reference [22].

The plan of the paper is as follows. In Section 2 we present the two-dimensional *t-t'-U* model and its properties. Within the framework of the COM, in Sections 3 and 4 we choose a suitable basic composite field and derive the expression of its propagator. In Section 5 we present the comparison of our analytical results for some local properties with numerical ones obtained by means of the quantum Monte Carlo method on a finite size lattice [2,30]. In Section 6 we show the results obtained for the structure of the energy bands, the shape of the Fermi surface and the relative position of the van Hove singularity with respect to the Fermi level as functions of the model parameters. We have paid particular attention to the comparison with the experimental data available for the superconducting cuprates. In Section 7 some conclusions are given.

2 The model

The two-dimensional *t-t'-U* model is described by the following Hamiltonian:

$$H = \sum_{ij} t_{ij}\, c^{\dagger}(i)\, c(j) + U \sum_{i} n_{\uparrow}(i)\, n_{\downarrow}(i) - \mu \sum_{i} n(i) \tag{2.1}$$

where $c^{\dagger}(i) = \left(c^{\dagger}_{\uparrow}(i), c^{\dagger}_{\downarrow}(i)\right)$ is the electron operator on the site i in the spinor notation, $n_{\sigma}(i)$ is the charge-density operator for the spin σ and $n(i)$ is the total charge-density operator. The hopping matrix t_{ij} has the following expression

$$t_{ij} = -4t\, \alpha_{ij} - 4t'\, \beta_{ij} \tag{2.2}$$

with

$$\begin{aligned} \alpha(\mathbf{k}) &= \frac{1}{2}\left[\cos(a\, k_x) + \cos(a\, k_y)\right] \\ \beta(\mathbf{k}) &= \cos(a\, k_x)\cos(a\, k_y) \end{aligned} \tag{2.3}$$

as Fourier transforms of α_{ij} and β_{ij}. These latter represent the projectors on the nearest and next-nearest neighbors, situated along the plaquette diagonals, respectively. a, the lattice constant, will be set to 1. The U parameter represents the intrasite Coulomb potential and μ the chemical potential. Throughout the paper, we will express all the energies in units of t and the latter will be set to 1.

This model does not enjoy the hole-particle symmetry owing to the presence of the t' term, that, under the hole-particle transformation $[c^{\dagger}(i) \rightarrow (-1)^{i} c(i)]$, changes its sign:

$$\mu\,(n, t') = U - \mu\,(2 - n, -t')\ . \tag{2.4}$$

3 The basic field

Let us introduce the following basic field:

$$\psi(i) = \begin{pmatrix} \xi(i) \\ \eta(i) \end{pmatrix} = \begin{pmatrix} (1 - n(i))\, c(i) \\ n(i)\, c(i) \end{pmatrix} \tag{3.1}$$

where the composite electron operators $\xi(i)$ and $\eta(i)$ represent the $n(i) = 0 \leftrightarrow 1$ and the $1 \leftrightarrow 2$ restricted electronic transitions, respectively. They make up the *so-called* Hubbard operator doublet $[c(i) = \xi(i) + \eta(i)]$. These two composite electron operators are well recognized to be responsible for the main distribution of the electron density of states for the Hubbard model from both analytical and numerical calculations [15].

The field ψ satisfies the following equation of motion obtained from the Hamiltonian (2.1):

$$\mathrm{i}\frac{\partial}{\partial t}\psi(i) = \begin{pmatrix} -\mu\xi(i) + \sum_j t_{ij} c\,(j) + \pi(i) \\ -\,(\mu - U)\,\eta(i) - \pi(i) \end{pmatrix} \tag{3.2}$$

where the operator π has the following form

$$\pi(i) = \sum_j t_{ij} \left(\frac{1}{2}\sigma^{\mu} n_{\mu}(i) c\,(j) + c(i)\left(c^{\dagger}\,(j)\,c(i)\right)\right). \tag{3.3}$$

The following definitions have been used

$$\sigma_{\mu} = (\mathbf{1}, \boldsymbol{\sigma}) \qquad \sigma^{\mu} = (-\mathbf{1}, \boldsymbol{\sigma}) \qquad n_{\mu}(i) = c^{\dagger}(i)\sigma_{\mu}c(i) \tag{3.4}$$

with $\mathbf{1}$ and $\boldsymbol{\sigma}$ being the unity and the three Pauli matrices respectively and $n_{\mu}(i)$ representing for $\mu = 0$ the total charge- and for $\mu = 1, 2, 3$ the spin- density operator for the site i. In equation (3.3) and in the ones that will follow the summation with respect to greek indices is understood.

4 The Green's function

The properties of the system are conveniently expressed in terms of the single particle retarded thermal Green's function:

$$S\,(\mathbf{k}, \omega) = \left\langle R\left[\psi(i)\psi^{\dagger}\,(j)\right]\right\rangle_{\mathrm{F.T.}} \tag{4.1}$$

where $\langle\ \ \rangle_{\mathrm{F.T.}}$ is the Fourier transform of the thermal average and $R[\ \ ]$ indicates the retarded time-ordered product. In the framework of the COM and neglecting finite life-time effects [19] we have

$$S\,(\mathbf{k}, \omega) = \frac{1}{\omega - m\,(\mathbf{k})\ I^{-1}\,(\mathbf{k}) + \mathrm{i}\delta} I\,(\mathbf{k})\,. \tag{4.2}$$

By considering a paramagnetic state with roto-translational invariance, $I(\mathbf{k})$ has the explicit expression:

$$I\,(\mathbf{k}) = \left\langle\left\{\psi(i), \psi^{\dagger}\,(j)\right\}\right\rangle_{\mathrm{F.T.}} = \begin{pmatrix} 1 - \frac{n}{2} & 0 \\ 0 & \frac{n}{2} \end{pmatrix} \tag{4.3}$$

n being the thermal average of the total charge-density operator $[n = \langle n(i)\rangle]$. Moreover, $m(\mathbf{k})$ is defined as

$$m\,(\mathbf{k}) = \left\langle \left\{ \mathrm{i}\frac{\partial}{\partial t}\psi(i), \psi^{\dagger}\,(j) \right\} \right\rangle_{\mathrm{F.T.}}. \tag{4.4}$$

From equation (4.4) direct calculations give

$$\begin{aligned} m_{11}\,(\mathbf{k}) = &-\mu\left(1 - \frac{n}{2}\right) - 4t\left[\Delta + \alpha\,(\mathbf{k})\,(1 - n + p)\right] \\ &- 4t'\left[\Delta' + \beta\,(\mathbf{k})\,(1 - n + p')\right] \end{aligned} \tag{4.5a}$$

$$\begin{aligned} m_{12}\,(\mathbf{k}) = m_{21}\,(\mathbf{k}) = &\ 4t\left[\Delta - \alpha\,(\mathbf{k})\left(\frac{n}{2} - p\right)\right] \\ &+ 4t'\left[\Delta' - \beta\,(\mathbf{k})\left(\frac{n}{2} - p'\right)\right] \end{aligned} \tag{4.5b}$$

$$\begin{aligned} m_{22}\,(\mathbf{k}) = &-(\mu - U)\,\frac{n}{2} - 4t\,(\Delta + \alpha\,(\mathbf{k})\,p) \\ &- 4t'\left[\Delta' + \beta\,(\mathbf{k})\,p'\right] \end{aligned} \tag{4.5c}$$

with

$$\Delta = \left\langle \xi^{\alpha}(i)\xi^{\dagger}(i)\right\rangle - \left\langle \eta^{\alpha}(i)\eta^{\dagger}(i)\right\rangle \tag{4.6a}$$

$$\Delta' = \left\langle \xi^{\beta}(i)\xi^{\dagger}(i)\right\rangle - \left\langle \eta^{\beta}(i)\eta^{\dagger}(i)\right\rangle \tag{4.6b}$$

$$\begin{aligned} p = &\frac{1}{4}\left\langle n_{\mu}^{\alpha}(i) n_{\mu}(i)\right\rangle \\ &- \left\langle \left[c_{\uparrow}(i)c_{\downarrow}(i)\right]^{\alpha} c_{\downarrow}^{\dagger}(i) c_{\uparrow}^{\dagger}(i)\right\rangle \end{aligned} \tag{4.6c}$$

$$\begin{aligned} p' = &\frac{1}{4}\left\langle n_{\mu}^{\beta}(i) n_{\mu}(i)\right\rangle \\ &- \left\langle \left[c_{\uparrow}(i)c_{\downarrow}(i)\right]^{\beta} c_{\downarrow}^{\dagger}(i) c_{\uparrow}^{\dagger}(i)\right\rangle. \end{aligned} \tag{4.6d}$$

We are using the following notation

$$\zeta^{\alpha}(i) = \sum_j \alpha_{ij}\zeta\,(j) \quad \zeta^{\beta}(i) = \sum_j \beta_{ij}\zeta\,(j)\,\cdot \tag{4.7}$$

The *internal* parameters Δ, Δ', p and p', as the chemical potential μ, have to be calculated in order to obtain the fermionic propagator as a function of the *external* parameters t, t', U, n and T (temperature). In the COM they are determined by solving a system of coupled self-consistent equations. Three equations come from the existing relations between the parameters n, Δ and Δ' and the Green's function matrix elements. The other two equations have been chosen in order to satisfy the Pauli principle at the level of matrix elements

$$\left\langle \xi(i)\eta^{\dagger}(i)\right\rangle = 0. \tag{4.8}$$

This last equation has been split in two by exploiting the independence of t and t' parameters.

5 The local properties and the comparison with numerical results

5.1 The chemical potential

We have calculated the chemical potential μ as a function of the external parameters using the system of self-consistent equations described in Section 4. We have compared our results with the ones obtained by means of the quantum Monte Carlo method [2] on a finite size lattice 8×8. The agreement is very good for $U = 4$ (cf. Fig. 1 of Ref. [29]).

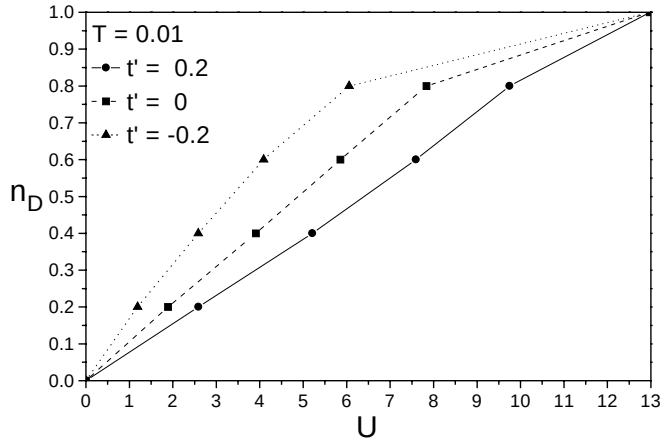

Fig. 1. Critical value of the filling n_D as a function of the intrasite Coulomb potential U for $T = 0.01$ and $t' = -0.2, 0, 0.2$.

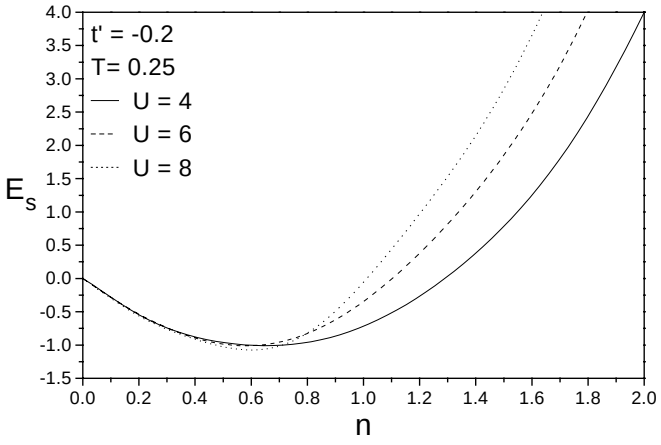

Fig. 2. Energy per site E as a function of the filling n for $t' = -0.2$, $T = 0.25$ and $U = 4, 6, 8$.

The quantum Monte Carlo data present a plateau for $n \approx 1.3$. This plateau is completely absent in our curve and is related to a finite size effect [31]. Moreover, the opening of the antiferromagnetic gap, due to a spin density wave instability [31], does not allow us to reproduce the behavior near half-filling where our solution is paramagnetic; this remark will also reflect on the comparison done with the double occupancy data.

5.2 The double occupancy

The double occupancy D, defined as the probability to have a couple of electrons ($\uparrow\downarrow$) on the same site, can be calculated through the following equation

$$D = \langle n_\uparrow(i) n_\downarrow(i) \rangle = \frac{1}{2} \left\langle \eta^\dagger(i) \eta(i) \right\rangle . \tag{5.1}$$

We have compared our results with the ones obtained by means of the quantum Monte Carlo method [2] on a finite size lattice 8×8 (cf. Fig. 3 of Ref. [29]). In the low-filling region our solution presents a characteristic feature, the existence of a critical value of the filling $n_D(U)$ before which the double occupancy is almost zero [$n \leq n_D(U)$]. The small residual is due to the thermal fluctuations. This kind of behavior seems to be absent in the quantum Monte Carlo data at finite temperature, but it might be inferred from the zero temperature data for the chemical potential [32]. We do not exclude the possibility that this feature could be an artifact of the two-pole approximation. Other analytical approaches do not exhibit such a behavior. See, for instance, reference [33] where a better agreement with the numerical data, as regards the behavior of the double occupancy as function of the filling, is found.

The explanation of this behavior of the double occupancy can be given as the existence of two regimes: one in which the low-filling let the carriers the possibility to move freely and avoid the high-energetic double occupancy of some sites and another one in which the number of carriers excludes the possibility to avoid the double occupancy. Obviously, this value of the filling, which marks the changing of regime, depends strongly on the value of the U and t' parameters, see Figure 1. As it should be expected, $n_D(U)$ increases by increasing U, owing to the larger energy needed to doubly occupy a site, and decreases by changing the sign of t' from negative to positive, owing to the resulting smaller mobility.

5.3 The energy per site

The internal energy per site E can be written as

$$E = K + V \tag{5.2}$$

where

$$K = \frac{1}{N} \sum_\sigma \sum_{ij} t_{ij} \left\langle c_\sigma^\dagger(i) c_\sigma(j) \right\rangle \tag{5.3a}$$

$$V = U \frac{1}{N} \sum_i \langle n_\uparrow(i) n_\downarrow(i) \rangle = UD \tag{5.3b}$$

are the kinetic and the potential energies, respectively.

The behavior of the internal energy per site E follows that of the kinetic energy K for low values of the filling, where the double occupancy is almost zero, whereas it follows that of the potential energy V for values of the filling greater than $n_D(U)$, see Figure 2. This can be easily inferred by looking at the U dependence: we have a very little dependence for any filling smaller than $n_D(U)$. This kind of behavior has been also found by means of quantum Monte Carlo method calculations [34,35] and slave-boson ones [36] giving a further confirmation about the presence of a region of the filling where the double occupancy has a very small value. To clarify this issue, other numerical data, in particular at lower temperatures are needed.

We can compute the internal energy through an alternative way. By introducing the Helmholtz free energy per site

$$F = E - TS \tag{5.4}$$

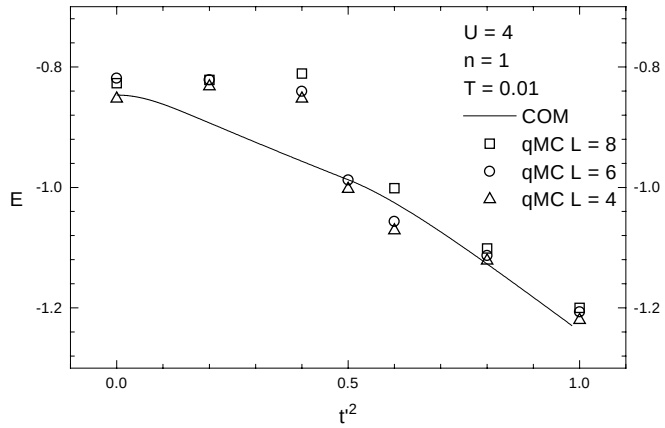

Fig. 3. Internal energy per site E as a function of $(t')^2$ for $n = 1$, $T = 0.01$ and $U = 4$.

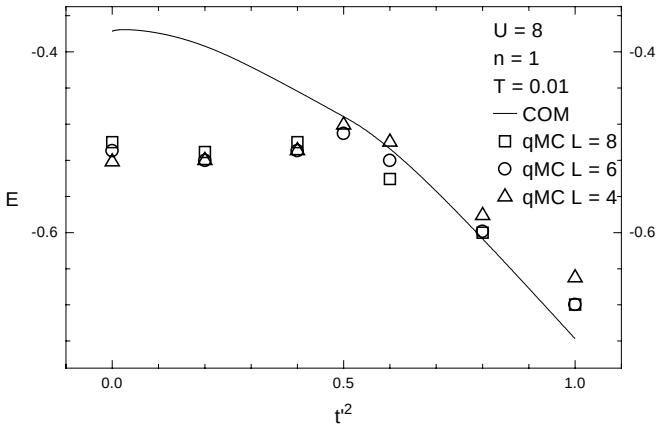

Fig. 4. Internal energy per site E as a function of $(t')^2$ for $n = 1$, $T = 0.01$ and $U = 8$.

where S is the entropy per site, from the Thermodynamics we have

$$S = -\frac{\partial F}{\partial T} \qquad \begin{cases} K' = -\dfrac{1}{4}\dfrac{\partial F}{\partial t'}\ \dfrac{\partial S}{\partial t'} = 4\dfrac{\partial K'}{\partial T} \\ \mu = \dfrac{\partial F}{\partial n} \qquad \dfrac{\partial S}{\partial n} = -\dfrac{\partial \mu}{\partial T} \end{cases} \tag{5.5}$$

where $K' = \left\langle c^{\dagger}(i)c^{\beta}(i)\right\rangle$. Then, it is straightforward to obtain the following formulas

$$F(T) = -4\int_0^{t'} K'(T)\ \mathrm{d}\tilde{t}' + \int_0^{n} \mu_{t'=0}(T)\ \mathrm{d}\tilde{n} \tag{5.6a}$$

$$S(T) = 4\int_0^{t'} \frac{\partial K'(T)}{\partial T}\ \mathrm{d}\tilde{t}' - \int_0^{n} \left.\frac{\partial \mu(T)}{\partial T}\right|_{t'=0}\ \mathrm{d}\tilde{n} \tag{5.6b}$$

$$E(T) = -4\int_0^{t'} \left(K'(T) - T\frac{\partial K'(T)}{\partial T}\right)\ \mathrm{d}\tilde{t}' + \int_0^{n} \left(\mu_{t'=0}(T) - T\left.\frac{\partial \mu(T)}{\partial T}\right|_{t'=0}\right)\ \mathrm{d}\tilde{n}. \tag{5.6c}$$

In this alternative scheme the thermodynamic quantities are all expressed through the single-particle Green's function. In principle both ways are equivalent to each other and must lead to the same results, but when approximations are involved, the situation drastically changes and different results can be obtained [37].

We have compared [37] these two schemes of calculation to each other (*i.e.*, comparing the values of the free energy) and with the numerical schemes (*i.e.*, Lanczos and quantum Monte Carlo). The results obtained by means of the alternative scheme usually correspond to a lower free energy. Moreover, they are by far in better agreement with the numerical data.

In this paper, we have compared our results, computed by means of the alternative scheme, with the ones obtained by means of the projector quantum Monte Carlo method [30] on a finite size lattice, see Figures 3 and 4. The agreement is very good in the region where $(t')^2$ is greater than 0.5 for both values of the U parameter. In the other region $[(t')^2 \leq 0.5]$ the spin density wave instability found by the authors does not allow us to reproduce the results. As it should be expected in a paramagnetic phase, the energy per site E lowers as $(t')^2$ increases owing to the consequential increment of the absolute value of the kinetic energy.

6 The single-particle properties and the description of the cuprates

In the framework of the COM, the Fourier transform of the single particle retarded thermal Green's function, see equation (4.2), may be rewritten as:

$$S(\mathbf{k},\omega) = \sum_{i=1}^{2} \frac{\sigma^{(i)}(\mathbf{k})}{\omega - E_i(\mathbf{k}) + \mathrm{i}\delta} \tag{6.1}$$

where $\sigma^{(1),(2)}(\mathbf{k})$ are given by

$$\sigma_{11}^{(i)}(\mathbf{k}) = \frac{I_{11}\left[2Q(\mathbf{k}) + (-)^{i+1}\,\Delta\Sigma(\mathbf{k})\right]}{4Q(\mathbf{k})} \tag{6.2a}$$

$$\sigma_{12}^{(i)}(\mathbf{k}) = \sigma_{21}^{(i)}(\mathbf{k}) = (-)^{i+1}\,\frac{m_{12}(\mathbf{k})}{2Q(\mathbf{k})} \tag{6.2b}$$

$$\sigma_{22}^{(i)}(\mathbf{k}) = \frac{I_{22}\left[2Q(\mathbf{k}) + (-)^{i}\,\Delta\Sigma(\mathbf{k})\right]}{4Q(\mathbf{k})} \tag{6.2c}$$

with

$$Q(\mathbf{k}) = \frac{1}{2}\sqrt{\left[U - \frac{m_{12}(\mathbf{k})}{I_{11}I_{22}}\right]^2 + 2nU\frac{m_{12}(\mathbf{k})}{I_{11}I_{22}}} \quad (6.3a)$$

$$R(\mathbf{k}) = \frac{1}{2}\left[U - 2\mu - 8t\alpha(\mathbf{k}) - 8t'\beta(\mathbf{k})\right] - \frac{1}{2}\frac{m_{12}(\mathbf{k})}{I_{11}I_{22}} \quad (6.3b)$$

$$\Delta\Sigma(\mathbf{k}) = (1-n)\frac{m_{12}(\mathbf{k})}{I_{11}I_{22}} - U. \quad (6.3c)$$

$E_{1,2}(\mathbf{k})$ represent the energy bands and have the following expressions:

$$E_i(\mathbf{k}) = R(\mathbf{k}) + (-)^{i+1}Q(\mathbf{k}). \quad (6.4)$$

According to this, the Fermi surface of the system may be defined as $E_2(\mathbf{k}) = 0$ and the electronic density of states, $N(\omega)$, may be computed through the following formula:

$$N(\omega) = \frac{1}{2\pi^2}\sum_{i,j,l=1}^{2}\int \mathrm{d}\mathbf{k}\,\sigma_{jl}^{(i)}(\mathbf{k})\,\delta\left[\omega - E_i(\mathbf{k})\right] \quad (6.5)$$

where the integration has to be performed over the first Brillouin zone. The presence of two bands gives a structure of the density of states characterized by two logarithmic van Hove singularities.

6.1 The energy bands and the van Hove singularity

Both band structure calculations and experiments generally find that the Fermi level is close to the van Hove singularity at the optimal doping (δ_c) for the majority of the multi-layer cuprate superconductors, like $YBa_2Cu_3O_{7-\delta}$ (YBCO), $Bi_2Sr_2Ca_1Cu_2O_\delta$ (Bi-2212) and Hg compounds [12,38,39].

In particular, for YBCO the relative distance (ΔE) between the Fermi level and van Hove singularity has been found to be within 6 meV for its optimal doping stoichiometric concentration [40] ($\delta_c^{\mathrm{YBCO}} \approx 0.15$).

For the electron-doped $Nd_{2-\delta}Ce_xCuO_4$ (NCCO), it has been found a value of ΔE of ≈ 200 meV for its optimal electron-doping concentration [41] ($\delta_c^{\mathrm{NCCO}} \approx 0.15$).

So far, the available photoemission results [42–44] for the $La_{2-x}Sr_xCuO_4$ (LSCO) agree with the experimental data for the static susceptibility [45], the electronic specific heat and the entropy [46] after which the van Hove singularity seems to coincide with the Fermi level at the critical doping (x_c) at which the superconductivity disappears ($x_c^{\mathrm{LSCO}} \approx 0.3$). A comprehensive discussion about this issue can be found in reference [21], where many experimental results for LSCO are reviewed and possibly explained within the framework of the COM.

More generally, the experimentally derived dispersions of the Cu-O plane anti-bonding bands for a series of cuprates (Bi-2212, YBCO, $Bi_2Sr_2CuO_\delta$ (Bi-2201), $YBa_2Cu_4O_8$, NCCO) show a remarkable similarity to one another with the van Hove singularity appearing near the Y-point $(0,\pi)$ of the Brillouin zone [47].

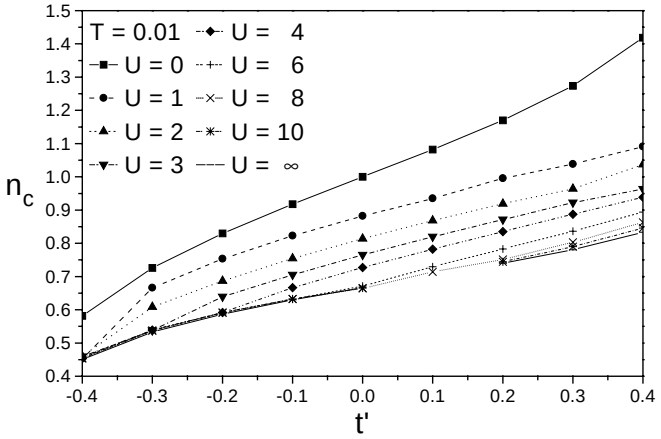

Fig. 5. Critical filling n_c as a function of the t' and U parameters for $T = 0.01$.

The value of the t' parameter is crucial in determining the structure of the energy bands and therefore the relative position of the van Hove singularity with respect to the Fermi level. The critical value of the filling ($n_c \doteq 1-\delta_c^{\mathrm{YBCO}} \doteq 1-x_c^{\mathrm{LSCO}}$) for which the van Hove singularity of the lower band coincides with the Fermi level, has the behavior shown in Figure 5 as a function of the t' and U parameters. n_c has been computed by studying the density of states, see equation (6.5), as a function of the filling n for fixed values of the t' and U parameters. Figure 5 contains a complete information about the structure and the doping evolution of the density of states and therefore permits a comprehensive comparison between the experimental situation and the physics described by the t-t'-U model. The primary, but absolutely not unique, effect of a positive (negative) value of t' is to lower (rise) the value of the energy at point Γ and along the line X-Y; as direct consequence, the number of available states in the lower Hubbard subband increases (decreases). This also explains the virtual rotation that the Fermi surface seems to perform as a function of t', for fixed values of doping and Coulomb interaction (see Fig. 8).

The critical value of the filling ($n_c' \doteq 1+\delta_c^{\mathrm{NCCO}}$), that corresponds to the coincidence of the upper band van Hove singularity with the Fermi level can be obtained by the one of the lower band through the following formula, that comes directly from the particle-hole symmetry

$$n_c'(U,t') = n_c(0,t') + n_c(0,-t') - n_c(U,-t'). \quad (6.6)$$

This critical value of the filling can be also interesting with respect to the electron-doped compounds for which the relevant band is the upper one.

We have studied the structure of the energy bands as function of the model parameters. The results have shown that it is possible to obtain a good agreement with the experimental data by choosing reasonable sets of parameters. In particular, the value of ΔE for NCCO together

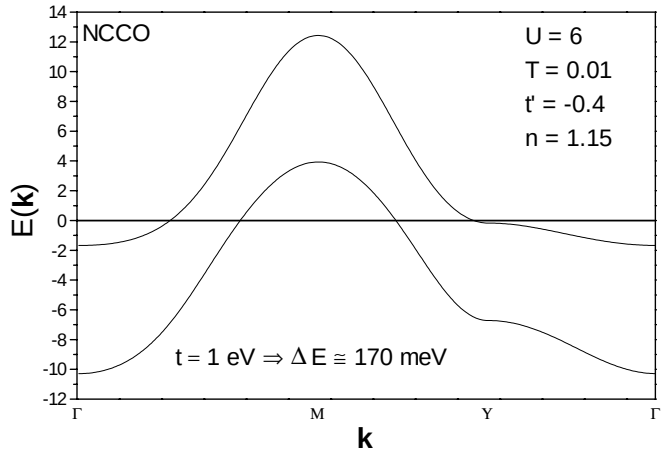

Fig. 6. Energy bands for $t' = -0.4$, $T = 0.01$, $n = 1.15$ and $U = 6$.

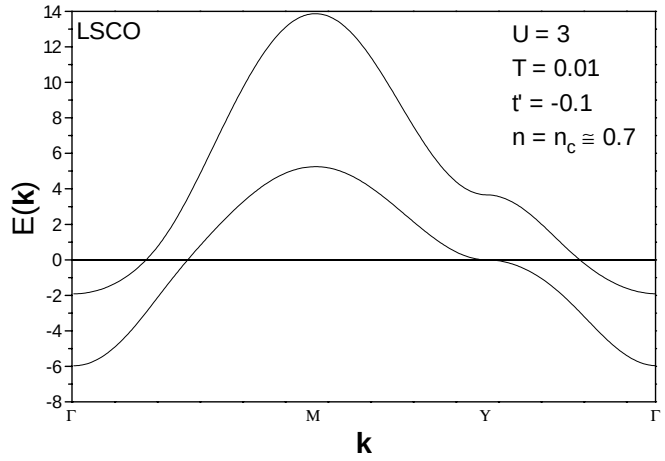

Fig. 7. Energy bands for $t' = -0.1$, $T = 0.01$, $n = 0.7$ and $U = 3$.

with the shape of the energy band can be obtained by the following set of parameters: $U = 6$, $t' = -0.4$, see Figure 6. In the case of LSCO, we can obtain the right value for x_c by using the following set of parameters: $U = 3$, $t' = -0.1$, see Figure 7. In this figure we can observe the coincidence between the van Hove singularity and the Fermi level as required by the LDA calculations [48] and experiments [42–46].

Finally, it can be easily seen from Figure 5, that it is impossible to obtain the features suggested for YBCO unless to use a set of parameters like: $U = 1$, $t' = -0.4$ with a value of the U parameter really too small in comparison with the band calculation results [5,6]. Moreover, even using this set of parameters, the relevant van Hove singularity results to be the upper band one, in strict contradiction with the hole-doped nature of the compound. This is due to the value of the t' parameter necessary to obtain the right bending of the Fermi surface after the ARPES data [49]. A value of -0.4 for the t' parameter gives a value for the critical filling of the lower band van Hove singularity too small with respect to the optimal doping concentration required by experimental data [49].

Independently to the chosen set of parameters the van Hove singularity appears at the Y-point as in the experiments.

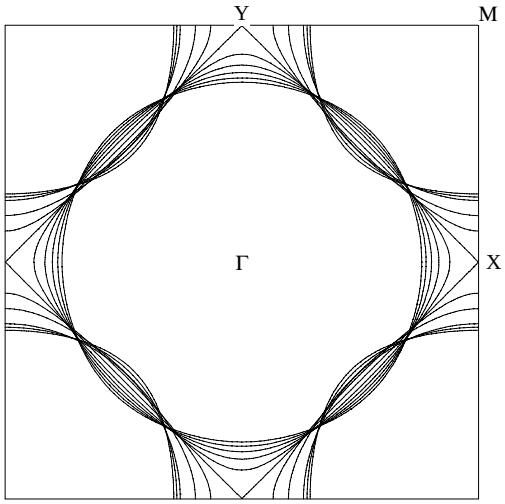

Fig. 8. FS for $t' = -0.5 \rightarrow 0.5$, $T = 0.01$, $n = 0.73$ and $U = 4$.

6.2 The Fermi surface

The Fermi surface of the various cuprates are remarkably similar one to another; in particular, photoemission experiments show a large Fermi surface for a series of cuprates at their optimal doping concentration [47] (Bi-2212, Bi-2201, NCCO, YBCO).

Photoemission studies of NCCO find a hole-like and roughly circular Fermi surface [41]. The apparent simplicity of this Fermi surface is deceptive, since the transport properties imply that the majority carriers are electron-like.

Photoemission [42–44] and positron annihilation [50] studies of the doping dependence of the Fermi surface for the LSCO are consistent with a pseudo-nested hole-like Fermi surface as predicted by LDA calculations [48] and found by the COM for the simple Hubbard model [21].

The shape and, in particular, the bending of the Fermi surface are strongly dependent on the value of the t' parameter. The bending is electron-like for positive values of t' and hole-like for negative ones, independently on the strength of the U parameter. This can lead for fixed values of filling n and of the U parameter to a real rotation of the Fermi surface by varying the value of the t' parameter. In Figure 8 we show the Fermi surface of the t-t'-U model with $U = 4$, $T = 0.01$ and $n \cong 0.73$ for values of the t' parameter that range from -0.5 to 0.5 with step 0.1. The chosen value of the filling corresponds to the critical value n_c for $t' = 0$. The Fermi surface is open and hole-like for $t' = -0.5$. It is nested for $t' = 0$. It is closed and electron-like for $t' = 0.5$. This gives the idea of a $\frac{\pi}{4}$ possible rotation that can be driven by the t' parameter.

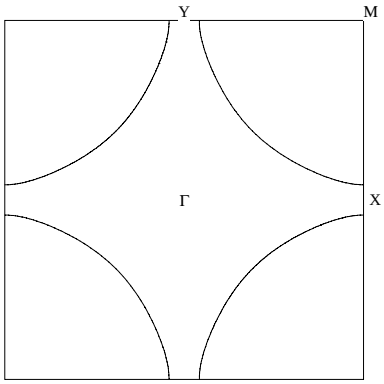

Fig. 9. FS for $t' = -0.4$, $T = 0.01$, $n = 1.15$ and $U = 6$.

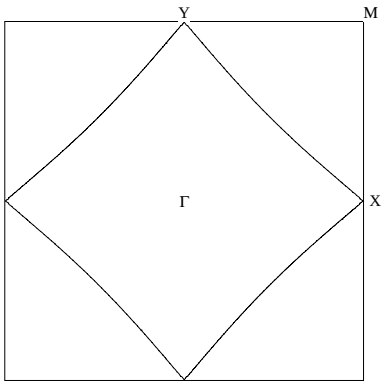

Fig. 10. FS for $t' = -0.1$, $T = 0.01$, $n = 0.7$ and $U = 3$.

The critical value of the filling for which the Fermi surface closes corresponds to the value for which the van Hove singularity of the lower band coincides with the Fermi level. The perfect nesting can be obtained only for a zero value of the t' parameter. Any non-zero value leads to a pseudo-nesting as the Fermi surface, although closed, conserves some bending.

It is really relevant that the experimentally observed Fermi surface for NCCO can be obtained, in our formulation, by the same set of parameters that gives a correct band dispersion, see Figure 9. Moreover, it has to be pointed out that the value of the t' parameter capable to reproduce the bending of the Fermi surface is in agreement with the one predicted by band calculations [2].

In the case of LSCO, the same set of parameters already used to successfully describe the band dispersions allows us to reproduce both the pseudo-nesting and the hole-like bending of the Fermi surface as found by the photoemission [42–44] and positron annihilation [50] experiments and LDA calculations [50,48], see Figure 10.

7 Conclusions

Nowadays, the experimental situation for many physical properties of cuprate high-T_c superconductors is well established. This imposes strong constrains on the theoretical models and/or adopted approximation schemes. The band dispersions and the Fermi surface of a large series of materials are today well-known.

We have studied the two-dimensional *t-t'-U* model, by means of the Composite Operator Method to analyze the possibility to handle the complexity of the experimental situation for the cuprates. Using relations containing the Pauli principle, we have been able to fix the dynamics in a fully self-consistent way. Furthermore, the recovery of the Pauli principle has assured us to satisfy the relations coming from the particle-hole transformation. To check our solution we have compared our results for the local quantities with the ones coming from numerical schemes with a very good agreement.

We have computed the structure of the energy bands, the shape of the Fermi surface and the relative position of the van Hove singularity. The comparison with experimental data has shown that the Hubbard model is capable to describe both $La_{2-x}Sr_xCuO_4$ and $Nd_{2-x}Ce_xCuO_4$, that share the property to be 1-layer cuprates. On the contrary, it does not seem the case for $YBa_2Cu_3O_{7-\delta}$ that is a 2-layer cuprate. This can be read as a clear signal that two-dimensional Hubbard-like models can play an important role in describing the physics of the 1-layer cuprates superconductors, but that the multi-layer ones need some more complex models.

In conclusion, the *t-t'-U* model emerges as a minimal model for 1-layer cuprate materials.

References

1. H. Monien, D. Pines, M. Takigawa, Phys. Rev. B **43**, 258 (1991).
2. D. Duffy, A. Moreo, Phys. Rev. B **52**, 15607 (1995).
3. D. Duffy, A. Moreo, Phys. Rev. B **55**, 12918 (1997).
4. D. Duffy *et al.*, Phys. Rev. B **56**, 5597 (1997).
5. L.F. Feiner, J.H. Jefferson, R. Raimondi, Phys. Rev. B **53**, 8751 (1996).
6. R. Raimondi, J.H. Jefferson, L.F. Feiner, Phys. Rev. B **53**, 8774 (1996).
7. T. Tohyama, S. Maekawa, Phys. Rev. B **49**, 3596 (1994).
8. R.J. Gooding, K.J.E. Vos, P.W. Leung, Phys. Rev. B **50**, 12866 (1994).
9. J. Bala, A.M. Oles, J. Zaneen, Phys. Rev. B **52**, 14597 (1995).
10. P. Bénard, L. Chen, A.M. Tremblay, Phys. Rev. B **47**, 15217 (1993).
11. Q. Si, T. Zha, K. Levin, J.P. Lu, Phys. Rev. B **47**, 9055 (1993).
12. D.S. Dessau *et al.*, Phys. Rev. Lett. **71**, 2781 (1993).
13. E. Dagotto, A. Nazarenko, M. Boninsegni, Phys. Rev. Lett. **73**, 728 (1994).
14. S. Uchida, Jpn J. Appl. Phys. **32**, 3784 (1993).
15. E. Dagotto, Rev. Mod. Phys. **66**, 763 (1994).
16. P.A. Lee, Phys. Rev. Lett. **63**, 680 (1989).
17. P.W. Anderson, Science **235**, 1196 (1987).
18. P. Fulde, *Electron Correlations in Molecules and Solids*, 3rd edn. (Springer-Verlag, Berlin Heidelberg New York, 1995).

19. F. Mancini, S. Marra, H. Matsumoto, Physica C **244**, 49 (1995).
20. A. Avella *et al.*, Int. J. Mod. Phys. B **12**, 81 (1998).
21. A. Avella, F. Mancini, D. Villani, Sol. Stat. Comm. **108**, 723 (1998).
22. A. Avella, F. Mancini, D. Villani, Phys. Lett. A **240**, 235 (1998).
23. A. Avella, F. Mancini, M. Sánchez, Europhys. Lett. **44**, 328 (1998).
24. F. Mancini, Phys. Lett. A **249**, 231 (1998).
25. F. Mancini, D. Villani, H. Matsumoto, Phys. Rev. B **57**, 6145 (1998).
26. L.M. Roth, Phys. Rev. **184**, 451 (1969).
27. W. Nolting, Z. Phys. **255**, 25 (1972).
28. J. Beenen, D.M. Edwards, Phys. Rev. B **52**, 13636 (1995).
29. A. Avella, F. Mancini, D. Villani, Physica B **230–232**, 912 (1997).
30. R.E. Hetzel, P. Topalis, 1997 (unpublished).
31. We thank Dr. D. Duffy for correspondance on this subject.
32. F. Mancini, S. Marra, H. Matsumoto, Physica C **250**, 184 (1995).
33. Vilk *et al.*, J. Phys. I France **7**, 1309 (1997).
34. A. Moreo *et al.*, Phys. Rev. B **41**, 2313 (1990).
35. E. Dagotto *et al.*, Phys. Rev. B **45**, 10741 (1992).
36. L. Lilly, A. Muramatsu, W. Hanke, Phys. Rev. Lett. **65**, 1379 (1990).
37. F. Mancini, H. Matsumoto, D. Villani, J. Phys. Studies **4**, 474 (1999).
38. R. S. Markiewicz, J. Phys. Chem. Sol. **58**, 1179 (1997).
39. A.A. Abrikosov, J.C. Campuzano, K. Gofron, Physica C **73**, 214 (1993).
40. K. Gofron *et al.*, Phys. Rev. Lett. **73**, 3302 (1994).
41. D.M. King *et al.*, Phys. Rev. Lett. **70**, 3159 (1993).
42. A. Ino *et al.*, Phys. Rev. Lett. **81**, 2124 (1998).
43. A. Ino *et al.*, J. Phys. Soc. Jpn **68**, 1496 (1999).
44. A. Ino *et al.*, Phys. Rev. B **62**, 4137 (2000).
45. J.B. Torrance *et al.*, Phys. Rev. B **40**, 8872 (1989).
46. J.W. Loram *et al.*, J. Phys. Chem. Sol. **59**, 2091 (1998).
47. Z.-X. Shen, D.S. Dessau, Phys. Rep. **253**, 1 (1995).
48. J.H. Xu, T.J. Watson-Yang, J. Yu, A.J. Freeman, Phys. Lett. A **120**, 489 (1987).
49. R. Liu *et al.*, Phys. Rev. B **45**, 5614 (1992).
50. R.H. Howell *et al.*, Phys. Rev. B **49**, 13127 (1994).